Mar Geophys Res
DOI 10.1007/s11001-007-9036-3

ORIGINAL RESEARCH PAPER

Constructing a 3D structural block diagram of the Central Basin in Marmara Sea by means of bathymetric and seismic data

Emin Demirbağ · Hülya Kurt · Doğa Düşünür · Kerim Sarıkavak · Suna Çetin

Received: 27 July 2006 / Accepted: 20 November 2007
© Springer Science+Business Media B.V. 2007

Abstract In this study we made a comparative interpretation of multibeam bathymetric and seismic reflection data with different resolutions and penetration properties collected in the Central Basin of the Marmara Sea. Our main objectives were (i) to investigate and compare the active tectonic deformation observed on the sea bottom and within the uppermost sedimentary layers to that of the deep-seated deformation within the limits of resolution and penetration of the available geophysical data and (ii) to build a three-dimensional (3D) block diagram of the active tectonic and buried features by means of a *sliced mapping technique*. In this approach, we produced slice maps of the active and buried structural features at selected depths and then combined them to form a 3D structural block diagram. Motivation for our work was to produce a 3D structural diagram to derive a more detailed image of the structural features in the Central Basin where there is no available 3D seismic data. The observations from the bathymetry and seismic data and developed 3D diagram support the presence of a through-going strike-slip fault that forms a rotational depression zone against a right-stepping strike-slip faulting causing a pull-apart basin in the Central Depression zone.

E. Demirbağ (✉) · H. Kurt · D. Düşünür
Jeofizik Mühendisliği Bölümü, Maden Fakültesi, İstanbul Teknik Üniversitesi, Maslak, 34469 Istanbul, Turkey
e-mail: demirbag@itu.edu.tr

K. Sarıkavak
Mineral Research and Exploration Directorate, Ankara, Turkey

S. Çetin
Turkish Scientific and Technological Research Council - Marmara Research Center, Kocaeli, Turkey

Keywords Marmara Sea · Central Basin · Active tectonism · Seismic reflection · Multibeam bathymetry

Introduction

Investigation of active faulting in the Marmara Sea has been an important research area since the last devastating earthquake of size $M_w = 7.4$ located at Gölcük-İzmit (western Turkey) along the dextral North Anatolian Fault (NAF) zone (Fig. 1a and b) occurred on 17.08.1999 (Barka 1999). This recent earthquake as well as historical ones in and around the Marmara Sea introduced a possibility of a future destructive earthquake, which is most likely to occur in the northern Marmara Sea (Parsons et al. 2000). Therefore, it is important to study the NAF zone in the Marmara Sea and to evaluate the possible extent of a future earthquake because the northern shores of the Marmara Sea are densely populated and the most industrialized provinces of Turkey (Fig. 1b). It is well known that there is a high possibility of occurrence of a damaging earthquake in the Marmara Sea from a probabilistic point of view (Parsons et al. 2000). This high possibility is based on historical seismicity (Ambraseys and Finkel 1990, 1991, 1995; Ambraseys and Jackson 2000), observed seismicity (Gürbüz et al. 2000; Sato et al. 2004), and recent mapping of submarine active tectonic features (Okay et al. 1999, 2000; Parke et al. 1999; Aksu et al. 2000; Imren et al. 2001; Le Pichon et al. 2001; Armijo et al. 2002; Yaltırak 2002; Demirbağ et al. 2003; Carton 2005).

Multibeam bathymetric and seismic reflection methods are the most suitable methods for investigating the active tectonic features in submarine environments. Therefore, extensive multibeam and seismic reflection surveys were carried out by different research groups, particularly in the

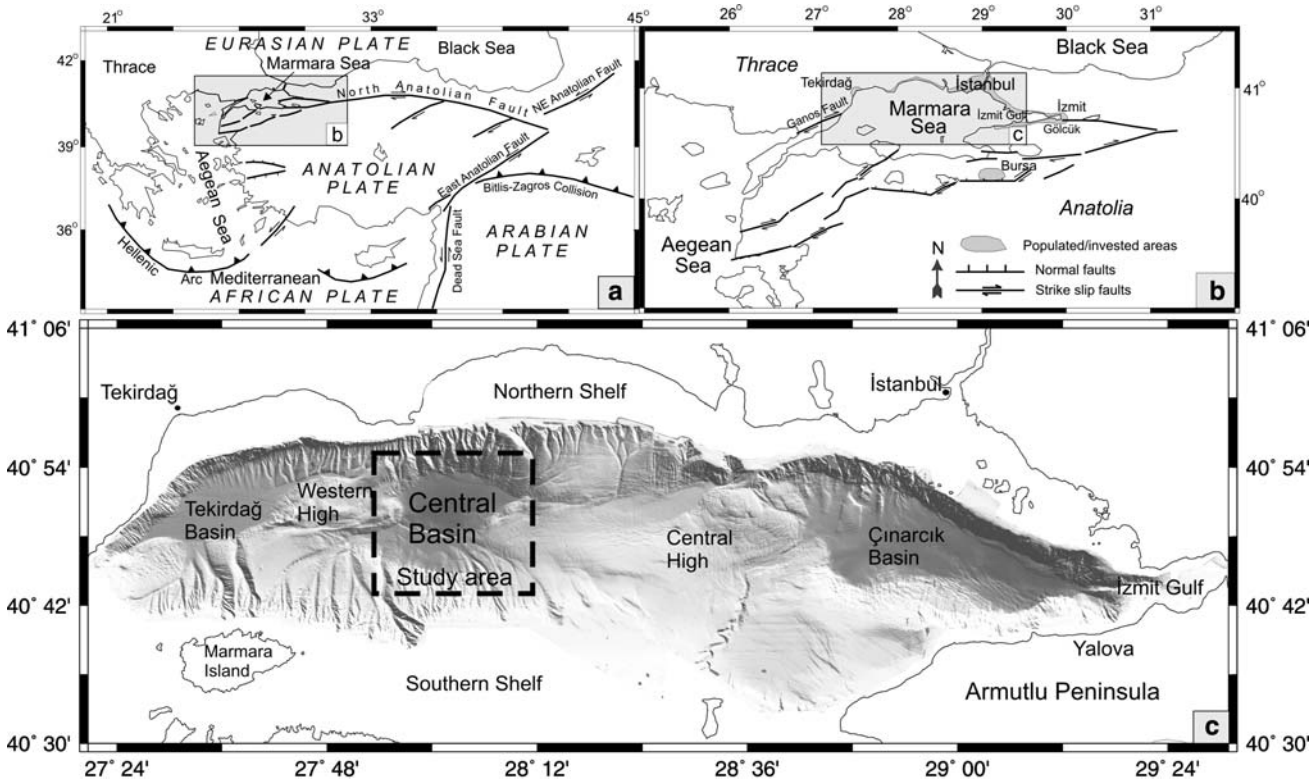

Fig. 1 Location map of the study area: (**a**) The North Anatolian and East Anatolian faults are the most important fault zones in the Anatolia. (**b**) Eastern Marmara Sea area is one of the most populated and industrially invested provinces of Turkey. (**c**) The Central Basin is one of the major basins in the Marmara Sea. An east–west oriented depression zone in the middle part of the Central Basin is noticed in the bathymetry

northern Marmara Sea by means of research vessel (R/V) of Mineral Research and Exploration Directorate (MTA) *R/V MTA Sismik-1* in 1997, 1999 and 2000, by *R/V Le Suroît* in 2000 and by *R/V Le Nadir* of French IFREMER in 2001. These data sets were studied by independent research groups during the last decade and results were published in the literature (Okay et al. 1999, 2000; Parke et al. 1999; Imren et al. 2001; Le Pichon et al. 2001; Armijo et al. 2002; Demirbag et al. 2003; Carton 2005). According to these studies, the dominant fault zone enters the Marmara Sea from İzmit Gulf in the east and follows the northern flank of the Çınarcık Basin. It extends westward and cuts the Central High to reach the Central Basin where it splays over a central deformation zone, before continuing westwards to cross the Tekirdağ Basin along the southern slopes and finally joins the Ganos Fault on land in the westernmost.

Two major but controversial interpretations are given for the recent evolution of the Central Depression zone in the Central Basin: according to Le Pichon et al. (2001) the Central Depression is formed by a single thoroughgoing strike-slip fault seated at seismogenic depths (shallower than 15 km in the Marmara Sea as discussed by Gürbüz et al. (2000) and causing a principal deformation zone in the uppermost sediments. Armijo et al. (2002) interpreted the same deformation zone as a pull-apart depression by right-stepping of the main fault branches. It is important to note that the depression zone in the Central Basin is between the 17.08.1999 earthquake fault (Gölcük-İzmit) in the east and the 09.08.1912 earthquake fault (Ganos) in the west. Therefore, the Central Depression zone is important in the sense that it is a key area for clarifying the style of deformation.

The recent studies summarized above are mostly based on one type of seismic reflection data in terms of resolution and penetration and the structural features are simply mapped on the bathymetry. In this study, we put together all available seismic data with different resolution and penetration to construct a three-dimensional (3D) structural block diagram. We used a *sliced mapping technique* in the Central Basin where 3D seismic data are not available. Our main objectives are to investigate the active tectonic deformation observed on the sea floor and within the uppermost sedimentary layers and compare to that of the mid to deep seated faults within the limits of resolution and penetration of available geophysical data. The motivation for our work is to put forward a 3D diagram of the structural features to derive a detailed model of the structural

features of the Central Basin, in particular the Central Depression zone.

Multibeam bathymetric data acquisition and mapping

In this study we used the multibeam bathymetric data collected by *R/V Le Suroît* in 2000. This data set is the most complete bathymetric data covering the northern Marmara Sea (Fig. 1c). It was collected using a Simrad EM300 multibeam echo-sounder with sonar frequency of 30 kHz. Processing of the raw data was carried out by the French institute IFREMER. Gridding and mapping of the data were obtained by means of Generic Mapping Tools (GMT) (Wessel and Smith 1995) and in-house developed software (Figs. 1c and 2). The multibeam data are adequate to make a bathymetric map of 1:50,000 scale (Rangin et al. 2001).

The average water depth of the Central Basin plain is 1150–1200 m. The basin plain is severely cut in the middle where the bathymetry deepens to about 1,250 m, forming the Central Depression zone. The northern slopes of the Central Basin are more pronounced with deep-cut, straight channels, whereas the southern slopes are gentle with wide, long valleys. Traces of the active faults are clearly observable in the bathymetric image maps generated by GMT mapping software. We generated gray scale shadow maps of the bathymetry by illuminating the gridded data from the main geographical directions. This approach allowed us to trace the active faults across the sea floor (Fig. 2). Note that the northern margin of the Central Depression zone consists of a series of bathymetric steps due to en échelon faults, whereas the southern margin shows more continuous fault traces with horse-tail splays.

Acquisition, compilation and processing of the seismic reflection data

In this study, we used three sets of seismic reflection data with different resolution and penetration (Tables 1–3). The first data set is the *R/V Le Suroît* surface-towed and deep-towed seismic data, which was used to map the active tectonic features within the uppermost sedimentary layers. This data set was collected by a bilateral cooperation

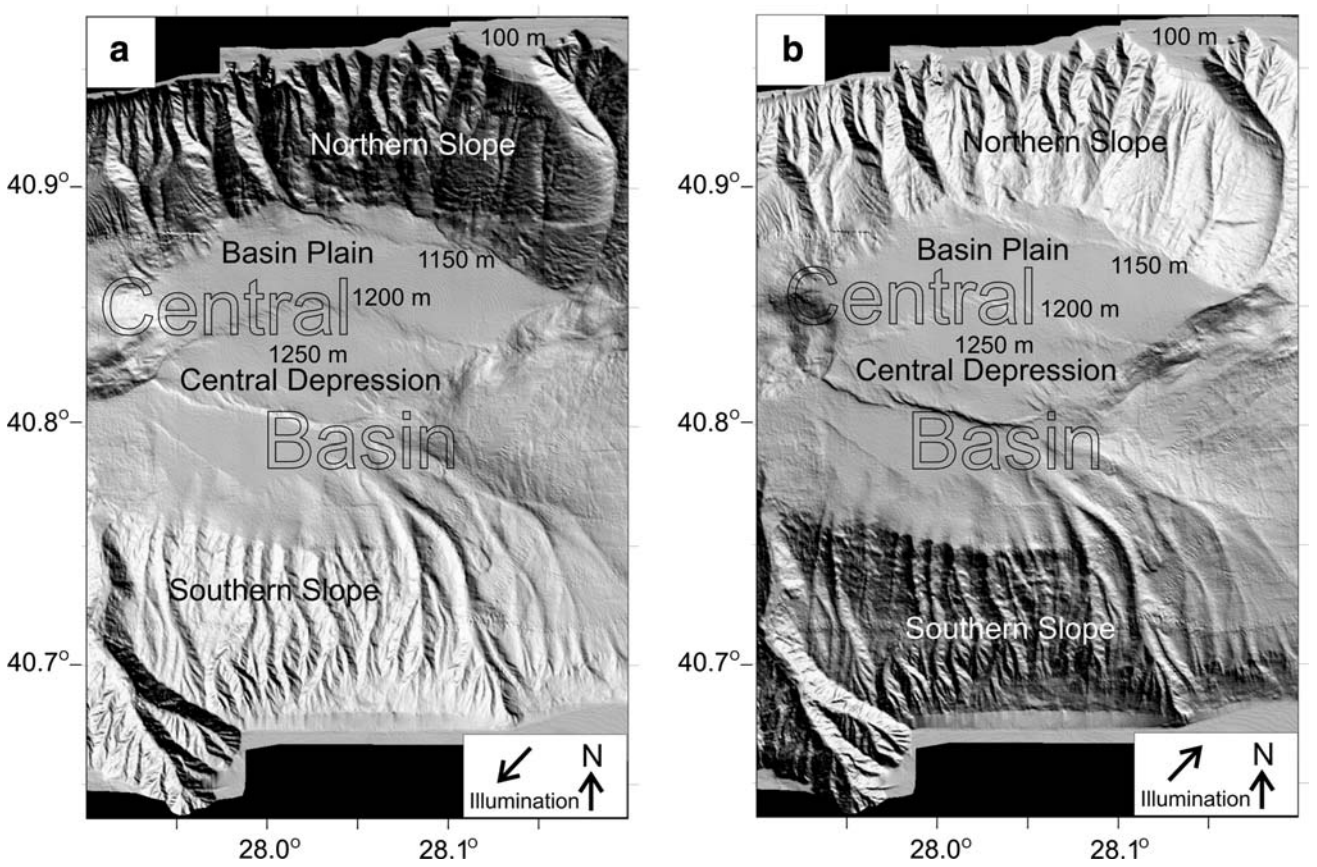

Fig. 2 Bathymetric image of the Central Basin. This map also constitutes the first slice in constructing the 3D block diagram. Note that the northern slopes are steep and cut by deep channels while the southern slope is gentler with longer valleys. The basin plain is located approximately at 1,200 m depth and sharply cut by 50 m or so deep scarps indicating active faults. (**a**) Illumination is from northeast. (**b**) Illumination is from southwest

Table 1 Seismic data collection parameters

Channels	Multi-channel			Single-channel	
Research vessel	MTA Sismik 1		*Le Nadir*	*Le Suroit*	
Survey and year	DMS 1997	M2S 2000	SeisMarmara 2001	Surface towed 2000	PASISAR 2000
Record length	6 s	6 s	12 s chopped	2 or 3 s	2 or 3 s
Sampling rate	2 ms	2 ms	4 ms	0.5 ms	0.5 ms
Number of channels	72	48	360	1	1
Source	Airgun	Airgun	Airgun	Sparker	Sparker
Shot interval	50 m	50 m	50 or 150 m	5 or 13 m	5 m
Offset	125 m	150 m	75 m	N/A	N/A
Station interval	12.5 m	12.5 m	12.5 m	N/A	N/A
Common depth point interval	6.25 m	6.25 m	6.25 m	N/A	N/A
Fold	9	6	45 or 15	N/A	N/A

N/A, Not applicable

Table 2 Seismic data processing steps

Channels	Multi-channel			Single-channel	
Research vessel	MTA Sismik 1		*Le Nadir*	*Le Suroit*	
Survey/year	DMS 1997	M2S 2000	Seismarmara 2001	Surface 2000	PASISAR 2000
Data transcribing	Yes	Yes	Yes	Yes	A special data processing flow is applied for this data set. Please refer to Savoye et al. (1995) and Demirbag et al. (2003) for more explanations.
Datuming to sea level	Yes	Yes	Yes	Yes	
Geometry def.	In-line	In-line	In-line	N/A	
Gain correction	Yes	Yes	Yes	Yes	
Filtering	Bandpass	Bandpass	Bandpass	Bandpass	
F-K filtering	No	No	Yes	N/A	
Sorting	Yes	Yes	Yes	N/A	
Velocity analysis	Yes	Yes	Yes	N/A	
NMO correction	Yes	Yes	Yes	N/A	
Muting	Yes	Yes	Yes	N/A	
Stacking	Yes	Yes	Yes	N/A	
Migration	Yes	Yes	Yes	N/A	

N/A, Not applicable

Table 3 Comparative analysis of the seismic data sets

Research vessel, type of seismic data and penetration versus resolution.	~Dominant frequencies (Hz) observed from the amplitude spectrum of the raw shot data and seismic source types	Calculated resolutions from Yılmaz (1987) for a sea bottom at 1,200 m depth and 1,500 m/s wave velocity		
		~Lateral (m)	~Vertical (m)	Resolution
Le Suroît single-channel, shallow penetration versus high resolution (PASISAR)	500 (3 kJ sparker)	<47	<1	High
Le Suroît single-channel, shallow penetration versus high resolution (surface-towed)	400 (3 kJ sparker)	47	1	High
MTA Sismik-1 multi-channel, moderate penetration and resolution	30 (10 or 9 airguns)	173	13	Moderate
Le Nadir multi-channel, deep penetration versus low resolution	10 (12 airguns)	300	36	Low

between French and Turkish scientific institutions in 2000. A second set of seismic reflection data was collected by *R/V MTA Sismik-1* in 1997 and 2000. The *R/V MTA Sismik-1* data set collected in 2000 is introduced for the first time during this study (Düşünür 2004). All of the data collected by *R/V MTA Sismik-1* provide a good look at the active structural features in moderate resolution and penetration in the Central Basin, particularly in the Central Depression. Using this data set, we are able to follow the active and buried structural features within the basin deposits and at the margins of the Central Basin. A third seismic data set is the deep penetration but low resolution data collected by *R/V Le Nadir* by bilateral cooperation between French and Turkish scientific institutes in 2001. This survey provides a deep image of the Central Basin.

R/V Le Suroît surface-towed seismic data were collected by using a 3 kJ sparker energy source and a single channel receiver. Most of the lines are oriented in a N–S direction (Fig. 3a). These data were mainly used by Le Pichon et al. (2001) to investigate the route of the NAF zone in the Marmara Sea. A second set of *R/V Le Suroît* data is the deep-towed seismic data collected simultaneously with the surface-towed data. This deep-towed data set is shortly called PASISAR (Seismic Passenger for Acoustic System Remorque/*Passenger Sismique du Système Acoustique Remorqué*; Savoye et al. 1995). The energy source was also a 3 kJ sparker towed at the surface, but the receiver was a deep-towed, single-channel streamer. Some of the PASISAR lines are oriented N–S to cross the E–W trending structural features, while some of the lines are collected in such a way that they cross the en échelon features on the sea floor along the northern and southern margins of the Central Depression zone (Fig. 3a). The sampling rate and record length are also the same as those used for the surface-towed data (Table 1). The PASISAR data are useful for investigation of active tectonism, particularly in the deep basins, by providing high resolution for a couple of hundred of meters depth below the basin plain. However, these data require unconventional data processing (Table 2) because of variable source-receiver geometry during data collection (Savoye et al. 1995). PASISAR data have been previously used to investigate the active faults in the Marmara Sea basins (Demirbağ et al. 2003).

The new multichannel seismic reflection data were collected by *R/V MTA Sismik-1* in 2000. A differential global positioning system (DGPS) was used for positioning. Seismic lines M2S-13, M2S-14, M2S-15, M2S-18 and M2S-19 crossing the Central Basin were used in this study. Most of these lines are oriented in a N–S direction (Fig. 3b) crossing the E–W oriented Central Depression zone in the middle of the Central Basin. The older data collected by *R/V MTA Sismik-1* in 1997 were studied by Imren et al. (2001) and were re-processed and re-interpreted in this study. We used seismic lines DMS-02, DMS-03, DMS-04 and DMS-05 located in the Central Basin from this data set (Fig. 3b). Lines M2S and DMS from the *R/V MTA Sismik-1* survey were processed in the Department of Geophysics, Istanbul Technical University. A conventional seismic data processing flow was applied to the data (Table 2). The resulting seismic sections were interpreted for basin-wide active structural features.

The seismic data collected by *R/V Le Nadir* in 2001 were provided by the Turkish Scientific and Technical Research Council (TÜBİTAK)-Marmara Research Center for our study (Table 1). Navigation was obtained by a DGPS system. We used seismic lines 3, 13, 14, 20, 46, and

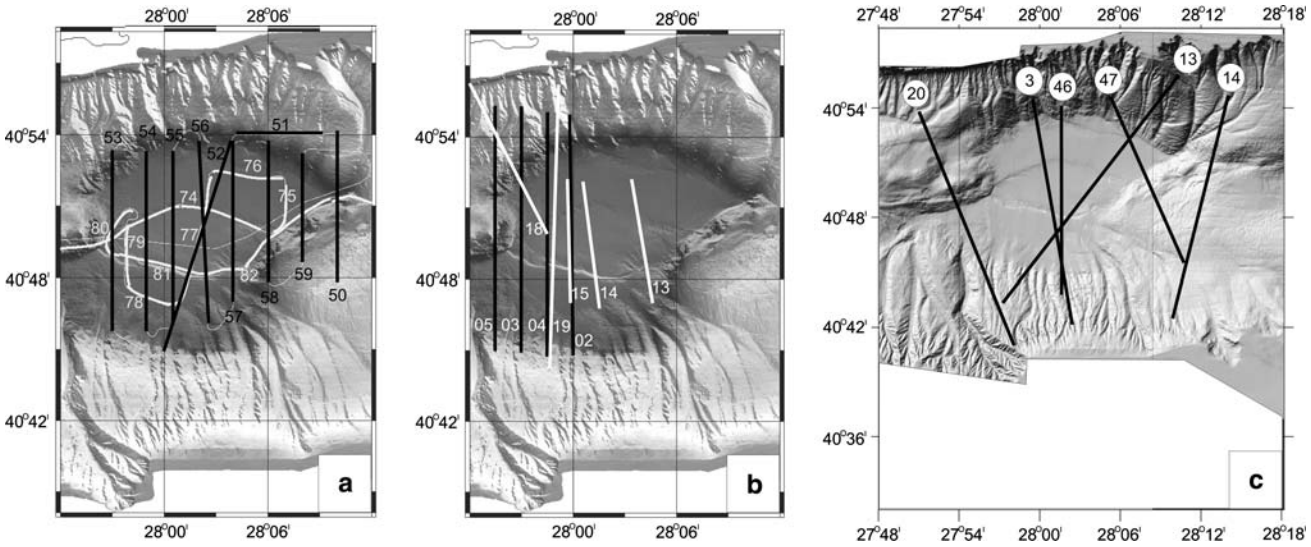

Fig. 3 Bathymetric image overlaid by the seismic lines in the Central Basin. They are from high-resolution/shallow-penetration to low-resolution/deep-penetration: (**a**) *R/V Le Suroît* lines: black lines are surface-towed and white lines are deep-towed (PASISAR) profiles (**b**) *R/V MTA Sismik-1* lines: black lines are DMS profiles and white lines are M2S profiles, (**c**) *R/V Le Nadir* lines

47 in this study (Fig. 3c). After data transcribing at TÜBİTAK-Marmara Research Center, further data processing were carried out in the Department of Geophysics at Istanbul Technical University. A conventional data processing stream was applied to the data (Table 2). During data processing, the record length was truncated at 12 s. Basin-wide, deep seated features were interpreted from the processed seismic sections.

Validity of the data in terms of resolution, penetration and geological targets

The seismic reflection data sets in this study can be classified into three categories in terms of penetration and resolution. Classification from "shallow penetration/high resolution" to "deep penetration/low resolution" is as follows: (i) the *R/V Le Suroît* single-channel surface-towed and PASISAR data (Le Pichon et al. 2001; Demirbağ et al. 2003) (ii) the *R/V Sismik-1* multichannel data (İmren et al. 2001; Düşünür 2004) and (iii) the *R/V Le Nadir* multichannel data (Carton 2005). Table 3 provides a comparative analysis of the resolution of the data presented in this article, and lists the vertical resolution and the first Fresnel zone (lateral resolution) at 1,200 m water depth (the average depth of the Central Basin) and for a P-wave velocity of 1,500 m/s for water. Note that the resolution values given in the table are for the seafloor and both the vertical and lateral resolution degraded as depth increased.

Multichannel seismic data provide good penetration, but are more complicated in terms of resolution. Both vertical (1/4 of dominant wavelength) and lateral (first Fresnel zone) arguments play a deterministic role in evaluating the resolution (Yılmaz 1987). The *R/V Le Suroît* data have the shallowest penetration, limited to a few hundred of meters from the sea floor, but with high vertical resolution of 1 m and a few tens of meters of lateral resolution (Table 1). This data set enables us to map the active tectonic features at shallow depths, particularly faults diverging upward. Small vertical steps are observable from the data, as well as branching of the minor faults and compressional effects in the sediments. Observation of small scale folds, faults and block rotations and their correlation with bathymetry can be carried out by means of this data set. The *R/V MTA Sismik-1* data have penetration of 3–4 km, sufficient for observing the active tectonics in terms of basin-wide faults. We are able to follow the active structural features within the deposits filling the Central Basin, as well as at the margins of the basin. However, faulting activity within the uppermost sedimentary layers and sea floor cannot be observed clearly from this data set due to limited resolution (Table 1). Small vertical offsets of the active faults on the sea bottom are smoothed out due to the Fresnel zone (Yılmaz 1987). *R/V Le Nadir* data provide the deepest penetration (>10 km), which is sufficient to observe the basin margin faults and base of the basin in some sections.

Interpretation of the seismic sections

Here we show typical examples of seismic sections and their interpretation for each set of the seismic data. Before we introduce the examples, we demonstrate the application scale, resolution and peneration differences in the data sets. For this purpose, three close seismic sections, section 55 from *R/V Le Suroit*, section M2S-14 from *R/V MTA Sismik-1* and section 3 from *R/V Le Nadir*, were selected (Fig. 3). We display these three seismic sections in the same horizontal and vertical scale to allow the reader to directly compare the sections in terms of resolution and penetration (Fig. 4).

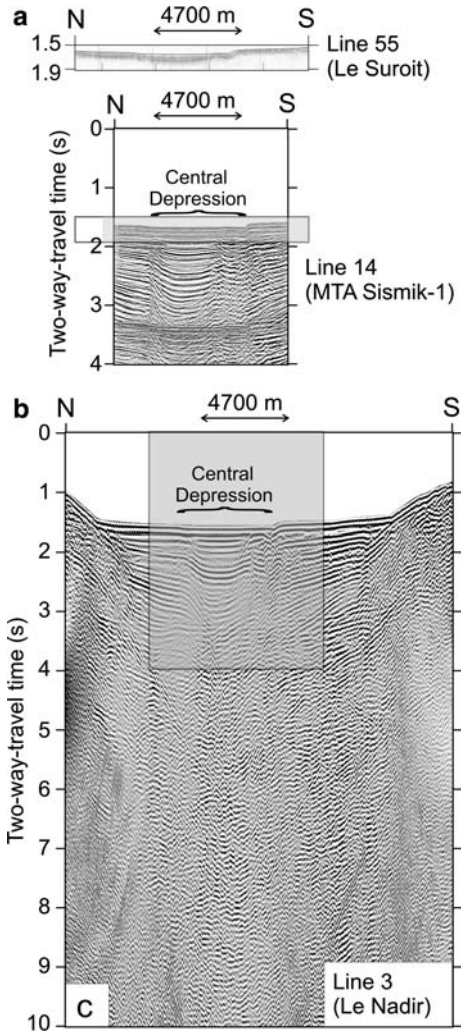

Fig. 4 Comparison of seismic data sets in terms of application scale, resolution and penetration. Section 55 from *R/V Le Suroit*, section M2S-14 from *R/V MTA Sismik-1* and section 3 from *R/V Le Nadir*. Refer to Fig. 3 for locations

To show the characteristic structural features of the study area, we take the first example from the *R/V Le Suroît* deep-towed PASISAR data, a N–S oriented section 79 located in the western part of the Central Basin (Figs. 3 and 5). As discussed above (see also Demirbağ, et al. (2003), the PASISAR data provide the best vertical resolution, but the shallowest penetration. This section displays approximately the upper 200 m of sediments at 1,200 m water depth. Section 79 clearly shows the active faults cutting the sea floor as well as the uppermost sediment layers. The sharp cuts in the sediments, particularly those at southern half of the section correlate well with the fault scarps observed on the bathymetry image (Fig. 2). For example, the steep scarp in the sea floor in the south is about 50 m high indicating that the faults are still quite active (Fig. 5). These faults are connected to the same main fault in the map plane (horizontal) although they appear to be different faults in the section plane (vertical) due to horse-tail splay. In the northern half of section 79, we observe small-scale structural features, including a small trough between the two sub-connecting minor faults, and compressed sediments in the uppermost levels. The small elevation of the bathymetry is remarkable. This group of small-scale, characterstic structural features are the surface and shallowest indicators of the northern boundary of the Central Depression zone.

We now show the N–S oriented *R/V MTA Sismik-1* seismic section M2S-19 as an example of moderate resolution and penetration data (Figs. 3 and 6). This section is important in the sense that it crosses the basin deposits, the

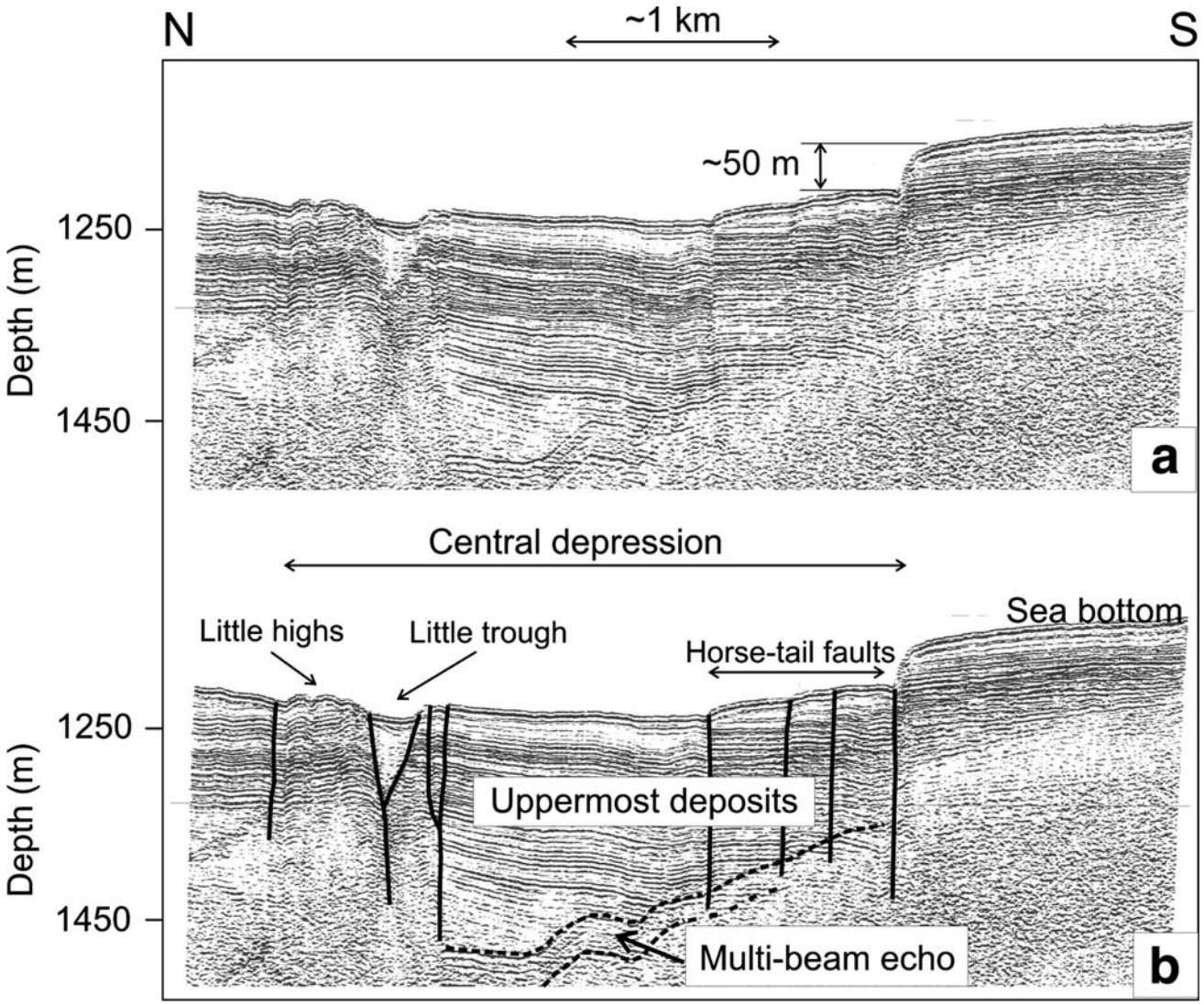

Fig. 5 (**a**) An example of single-channel shallow seismic section (Line 79) with high resolution from *R/V Le Suroît* and (**b**) its interpretation. Refer to Fig. 3 for line location. Very high resolution but shallow penetration provides clear images of the active structural features. The vertical axis is in meters. Note that the faults cut thin sedimentary layers as well as the sea bottom. Sharp scarps in the bathymetry and compressed young deposits are indications of active deformation

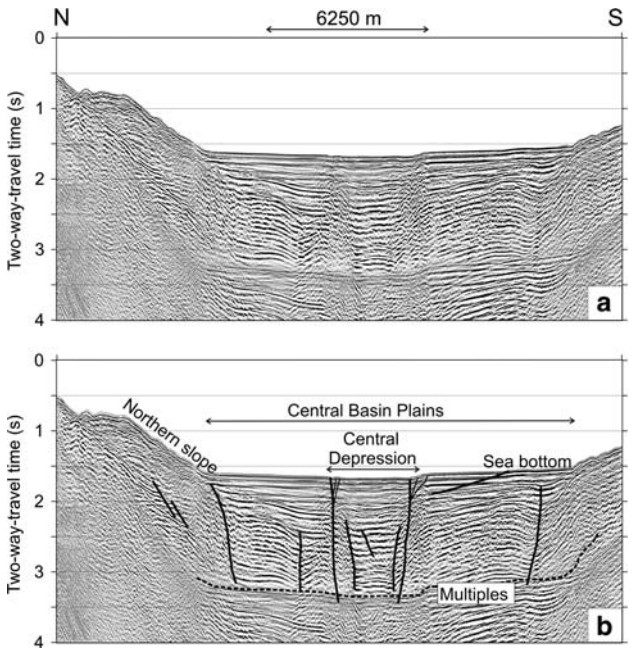

Fig. 6 (**a**) An example of multi-channel seismic section (Line M2S-19) with moderate penetration and resolution from *R/V MTA Sismik-1* and (**b**) its interpretation. Refer to Fig. 3 for line location. The penetration is well enough to observe the basin-wide structural features in expense of high resolution. Although the bathymetric scarps indicating active faults are not well observed in the section, the deformation in the sedimentary fill is well exposed to distinguish between the active and inactive basin-wide structures

structural features on the basin margins, and the Central Depression zone. It is interpreted between the sea floor reflections and the multiple reflections to avoid mis-interpretation below the multiples. The sea bottom reflections show undulated topography and a steep slope on the northern part of the section. The sea floor is quite smooth and almost horizontal in the basin plain, except where it is sharply cut by structural features of the Central Depression, such as the active faults bordering the depression. However, sharp bathymetric scarps are not recognized as well as in the PASISAR sections because of the limited vertical resolution.

The active faults forming the Central Depression zone are noticable before they are masked by the sea floor multiple reflections and they are most likely to continue to deeper parts of the basin. It is possible to distinguish the upward branches of the northern as well as southern fault. A few branches of these faults are observed at shallow levels but are connected at around 2 s depth (two-way travel time (TWT)). The branching of the faults towards the sea floor can be correlated to the en échelon fault scarps observed as a lineament on the bathymetric image map (Fig. 2).

Another important observation is that the faults at the margins of the Central Basin are not active like the ones forming the Central Depression zone. Note that the marginal basin faults are inactive, in that they do not cut the uppermost sedimentary layers. However, those sedimentary layers at 2.0 s or deeper appear to be affected by the basin margin faults (Fig. 6). Four other important structural features are also observable: three of which are within the Central Depression zone. However, these faults do not cut the uppermost sedimentary layers. The fourth fault is observed to the north of the Central Depression zone. This fault also does not cut the uppermost sedimetary layers. In the northern part of the section, there are two normal faults providing a stepwise lowering of the basin deposits in that region. The other seismic sections of *R/V MTA Sismik-1* show similar structual features and basin fill properties.

The last example is taken from a deep-penetrating, low-resolution seismic section of *R/V Le Nadir*. Section 13 provides a deep image of the Central Basin and the Central Depression zone, but with very low resolution (Figs. 3 and 7). It is not easy to observe the active fault scarps in the bathymetry due to very low resolution. However, it is important to note that the base of the Central Basin is observable on the section. This observation shows that the sedimentary fill is about 3 s TWT thick in the Central Basin. By using 1,500 m/s wave propagation velocity in the water and 2,600 m/s average velocity from the velocity analysis, the base of the Central Basin is estimated at approximately 5,850 m depth and with a sedimentary fill of about 4,725 m. The basins in the Marmara Sea are the products of a superimposed evolutionary history defined by two different aged fault systems: the early Miocene-early Pliocene Thrace-Eskişehir Fault Zone and its branches, and the late Pliocene-Recent North Anatolian Fault and its branches (Yaltırak 2002). Therefore, the age of basin fill should be Miocene-Pliocene for deep seated sediments and Quaternary to recent for shallow sediments.

The structural features are observable both at basin margins and at the borders of the Central Depression zone. The faults at the basin margins, particularly the southern one appear inactive while those forming the Central Depression deform the basin deposits from the sea floor to greater depths. It is possible that the northern and southern boundry faults of the Central Depression zone are joining at greater depths; but this is not clear from the section due to weak reflection continuity and reduced signal-to-noise ratios at depth.

Constructing a 3D block diagram and its evaluation

To form a 3D structural block diagram of the Central Basin, in particular the Central Depression zone, we developed an approach to map the structural features observed in the bathymetric image map and in the seismic sections. We produced "slice maps" of the structures at "feature sampling depths" from the bathymetric image

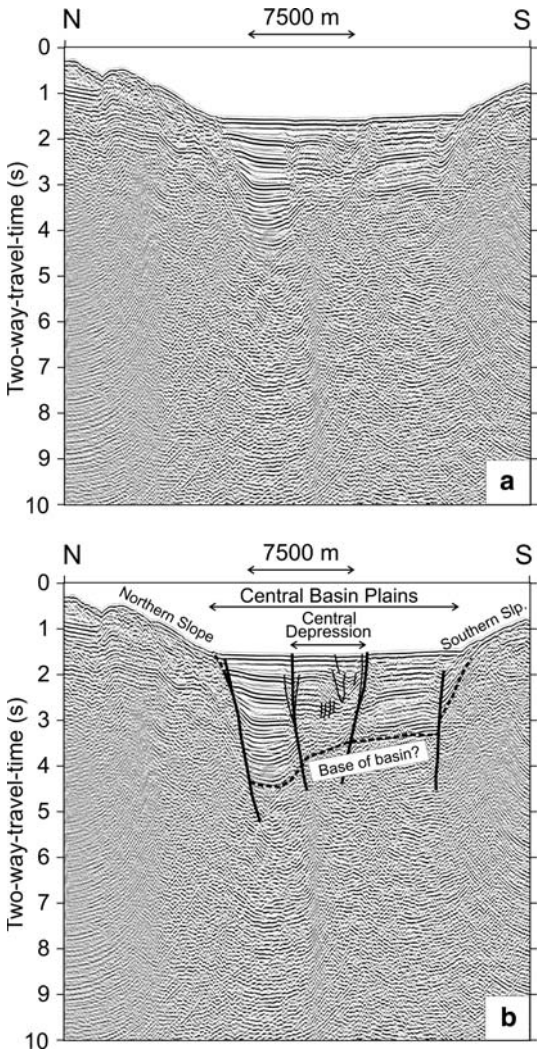

Fig. 7 (**a**) An example of multi-channel deep seismic section (Line 13) with low resolution from *R/V Le Nadir* and (**b**) its interpretation. Refer to Fig. 3 for line location. Note that details are totally lost due to very low resolution. However, deep penetration allows to observe possible base reflections of the Central Basin along the section. The basin deposits are thoroughly cut by the faults bordering the Central Depression zone from sea bottom to greater depths

map and seismic sections and then combined them to form the 3D block diagram (Fig. 8). We selected three levels of the "feature sampling depths" as follows: the sea floor is the first sampling level for scarps of the active faults; the second and third levels are at 2.0 and 3.0 s two-way-travel times in the multichannel seismic data, corresponding to 2.4 and 3.9 km depths, respectively. This approximation allowed us to determine the dip of the fault planes, and to check the continuity of the fault scarps observed at the sea bottom to deeper part of the sedimentary layers. In doing so, we are able to test whether some of these scarps were only surficial features, or if they connected to faults at greater depths in the basin.

We prefer to include only those features about which we are sure concerning their continuation in the seismic sections. The buried faults are shown in Fig. 8a whereas the active ones cutting the uppermost sediments and sea floor are shown in Fig. 8b. The sea bottom is the first level of slice mapping. The surficial response to active tectonism is well marked on the bathymetry and this correletes with the near surface response obtained from the PASISAR seismic data. The en échelon pattern and horse-tail splay of the active faults on the bathymetry, as well as at shallow subseafloor depths are clearly displayed in the diagram. The *R/V MTA Sismik-1* data provides a good check whether the surface features were indeed faults, or they were only surface features with no deeper extension. Extension of the faults to greater depths were accomplished by use of *R/V Le Nadir* data. These controlled and correlative interpretations generated the 3D structural block diagram seen in Fig. 8c.

The diagrams are projected to provide a view from the southeast (Fig. 8). The eastern and western, deep, straight main fault branches were included from Le Pichon et al. (2001). These faults are connecting to the Central Depression, which is delineated by en échelon faults along the northern border while the horse-tail splays are limited to the southern border. Both northern and southern fault distributions are connected to the basin-wide faults at greater depths as shown in Fig. 8. The genetic relation between the deeper basin-wide faults and shallow en échelon and horse-tail splays are obvious from the diagram. This way of imaging the structural features provides a better understanding of the structural model where there is no 3D seismic data available. Conventional structural evaluations are mostly based on faults mapped at the surface, and where the deep extension and curvature of the faults are usually omitted. However, the depth extension and curvature of a fault plane could be an important factor to asses the structural features. A surface map obtained from a single type of seismic data will not provide enough information such as slope, curvature and branching of the fault plane. In conclusion, a 3D block diagram obtained from a various type of seismic data with different resolutions and penetrations may provide improved insight into the evaluation of the structural features.

Evaluation of the 3D structural diagram (Fig. 8) in terms of two major but controversial interpretations (Le Pichon et al. 2001; Armijo et al. 2002) may be given as follows: en échelon faulting and horse-tail splays are mainly observed in the uppermost basin fill along the borders of the Central Depression zone. These surface-shallow sedimentary structural features join to each other and/or to basin-wide faults cutting through the sedimentary fill at both the northern and southern borders, thus forming the Central Depression zone. Slight convergence of the

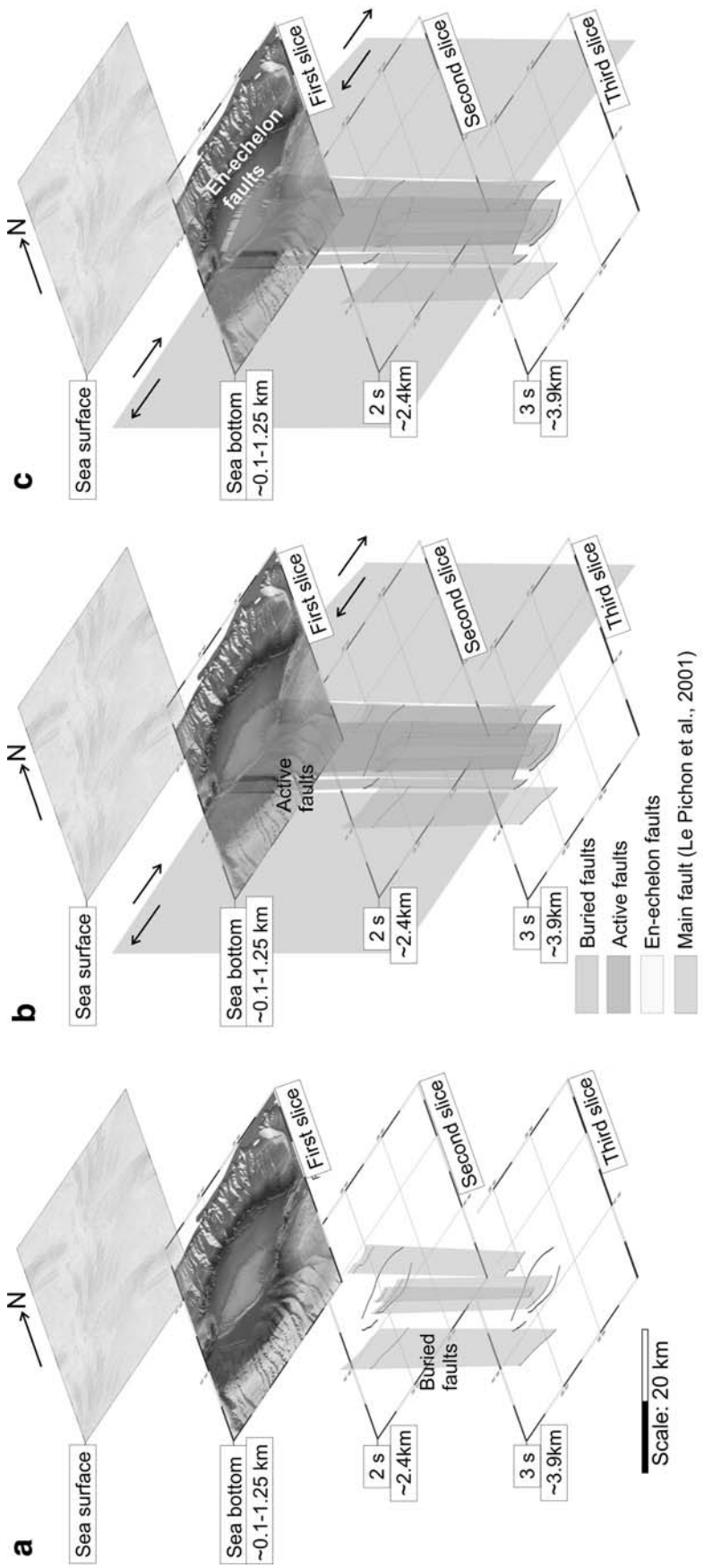

Fig. 8 3D structural block diagram. The structural features are presented in more detail from greater depths to the sea bottom as governed by the resolution of the available seismic data. (**a**) Buried structural features, (**b**) active structural features, (**c**) shallow en échelon and horse tail structural features together with buried and active faults. The strike slip main fault branches are from Le Pichon et al. (2001). The diagrams are viewed from southeast. Vertical exaggeration is about 20

northern and southern faults in section view and their continuation from east to west in plan view make it possible that these faults join to one another and/or to a larger fault at greater depths. Thus, the Central Depression zone along the two main dextral branches rotates clockwise by forming an en échelon system at the northern boundary and horse-tail splays at the southern boundary within the uppermost sedimentary layers.

It is well known that a depression zone is develeped in a strike slip system where two main branches of a strike slip fault have offset over a zone. The depression is mainly developed by normal faults oblique to the main strike slip branches. Unlike a pull-apart system, the Central Depression zone in the Central Basin lacks normal faulting distributed oblique to the main strike-slip branches. These observations from the bathymetry and seismic data, as shown in our 3D diagram support a tectonic model of a thoroughgoing strike-slip fault causing a rotational depression zone (Le Pichon et al. 2001) against a right-stepping strike slip faulting causing a pull-apart basin (Armijo et al. 2002).

Acknowledgements This study was supported by TÜBİTAK (Grant No: 102Y105). We thank the captains and crew members of *R/V MTA Sismik-1*, *R/V Le Suroît* and *R/V Le Nadir* for their effort during data acquisition. We thank the scientists and staff from Turkish institutes TÜBİTAK, MTA and SHOD, and from French institutes CNRS, INSU and IFREMER for collaborative work. We thank Drs. Celal Şengör, Naci Görür, Xavier Le Pichon, Alfred Hirn and Rolando Armijo for leading bathymetric and seismic data acquisition in the last decade in the Marmara Sea. We thank Drs. Haluk Eyidoğan, Ruhi Saatçılar, Semih Ergintav and Yavuz Hakyemez for their support to realize this study.

References

Aksu AA, Calon TJ, Hiscott RN, Yaşar D (2000) Anatomy of the North Anatolian Fault Zone in the Marmara Sea, western Turkey: extensional basins above a continental transform. GSA Today 10(6):3–7

Ambraseys NN, Finkel CF (1990) The Marmara Sea earthquake of 1509. Terra Nova 2:167–174

Ambraseys NN, Finkel CF (1991) Long-term seismicity of İstanbul and of the Marmara Sea. Terra Nova 3:527–539

Ambraseys NN, Finkel CF (1995) The seismicity of Turkey and adjacent areas—A historical review. Eren, İstanbul

Ambraseys NN, Jackson JA (2000) Seismicity of the Sea of Marmara (Turkey) since 1500. Geophys J Int 141:F1–F6

Armijo R, Meyer B, Navarro S, King G, Barka A (2002) Asymmetric slip partitioning in the Sea of Marmara pull-apart: a clue to propagation processes of the North Anatolian Fault? Terra Nova 14:80–86

Barka A (1999) The 17 August 1999 İzmit earthquake. Science 285:1858–1859

Carton H (2005) Three-dimensional seismic images of an active-pull apart basin: the Çınarcık Basin along the North Anatolian Fault. Lithos Sci Rep 7:63–72

Demirbağ E, Rangin C, Le Pichon X, Şengör AMC (2003) Investigation of the tectonics of the Main Marmara Fault by means of deep towed seismic data. Tectonophysics 361:1–19

Düşünür D (2004) Investigation of the active tectonism in the Central Marmara Basin by geophysical means. Master of Science Thesis (in Turkish with expanded abstract in English), Institute of Science and Technology, Istanbul Technical University

Gürbüz C, Aktar M, Eyidoğan H, Cisternas A, Haessler H, Barka A, Ergin M, Türkelli N, Polat O, Üçer SB, Kuleli S, Barış S, Kaypak B, Bekler T, Zor E, Biçmen F, Yörük A (2000) The seismotectonics of the Marmara region (Turkey): results from a microseismic experiment. Tectonophysics 316:1–17

İmren C, Le Pichon X, Rangin C, Demirbağ E, Ecevitoğlu B, Görür N (2001) The North Anatolian Fault within the Sea of Marmara: a new interpretation based on multi-channel seismic and multi-beam bathymetry data. Earth Planet Sci Lett 186:143–158

Le Pichon X, Şengör AMC Demirbağ E, Rangin C, İmren C, Armijo R, Görür N, Çağatay N, Mercier de Lepinay B, Meyer B, Saatçılar R, Tok B (2001) The active Main Marmara Fault. Earth Planet Sci Lett 192:595–616

Okay AI, Demirbağ E, Kurt H, Okay N, Kuşçu I (1999) An active, deep marine strike-slip basin along the North Anatolian Fault in Turkey. Tectonics 18:129–147

Okay AI, Kaşlılar-Özcan A, İmren C, Boztepe-Güney A, Demirbağ E, Kuşçu I (2000) Active faults and evolving strike-slip basins in the Marmara Sea, northwest Turkey: a multichannel seismic reflection study. Tectonophysics 321:189–218

Parke JR, Minshull TA, Anderson G, White RS, McKenzie DP, Kuşçu I, Görür N, Şengör AMC (1999) Active faults in the Sea of Marmara, western Turkey, imaged by seismic reflection profiles. Terra Nova 11:223–227

Parsons T, Toda S, Stein R, Barka A, Dieterich J (2000) Heightened odds of large earthquakes near Istanbul: an interaction-based probability calculation. Science 228:661–665

Rangin C, Demirbağ E, İmren C, Crusson A, Normand A, Le Drezen E, Le Bot A (2001) Marine Atlas of the Sea of Marmara (Turkey). 11 plates and 1 booklet. Special publication (ISBN 2-84433-068-1) by IFREMER Technology Center, Brest, France

Sato T, Kasahara J, Taymaz T, Ito M, Kamimura A, Hayakawa T, Tan O (2004) A study of microearthquake seismicity and focal mechanisms within the Sea of Marmara (NW Turkey) using ocean bottom seismometers (OBSs). Tectonophysics 391:303–314

Savoye B, Leon P, De Roeck YH, Marsset B, Lopes L, Herveou J (1995) PASISAR: a new tool for near-bottom very high resolution profiling in deep water. First Break 13:253–258

Wessel P, Smith WHF (1995) New version of the Generic Mapping Tools released. EOS Trans. AGU 76:329

Yaltırak C (2002) Tectonic evolution of the Marmara Sea and its surroundings. Mar Geol 190:493–529

Yılmaz Ö (1987) Seismic data processing. Investigations in Geophysics, vol 2. Society of Exploration Geophysicists, Tulsa, Oklahoma